M$^{\text{odeling}}$ M C$^{\text{omputing}}$ $_{\text{athematical}}$

Analytical images of Kepler's equation solutions and their applications

Vavrukh M., Dzikovskyi D., Stelmakh O.

Ivan Franko National University of Lviv,
8 Kyrylo and Methodiy Str., 79005 Lviv, Ukraine

The simple fast-converging analytical calculations algorithms for eccentric anomaly are proposed for an arbitrary eccentricity $0 < e \leqslant 1$. The kinematic characteristics of Halley's comet are calculated as the function of time. Mass of Galaxy + NGC 224 system using the model of elliptical relative motion is also estimated.

1. Introduction

It's well known from the celestial mechanics, the relative motion of two point gravitating bodies system with masses m_1 and m_2 occurs by Keplerian orbits

$$r = p\{1 + e \cos v\}^{-1}, \tag{1}$$

where r and v are polar coordinates, and the focal parameter p and eccentricity e are determined by the masses of bodies and integrals of motion — angular momentum l and energy $\mathscr{E}$ (see [1]):

$$p = l^2 \mu^{-2} K^{-1}, \quad e = \{1 + 2\mathscr{E} l^2 \mu^{-3} K^{-2}\}^{1/2}. \tag{2}$$

$K = G(m_1 + m_2)$ is the so-called gravitational parameter, G is the gravitational constant, $\mu = m_1 m_2 (m_1 + m_2)^{-1}$. Using expression for the angular momentum $l = r^2 \mu \, dv/dt$ (where t is time), equation of the orbit (1) and expression for p from equations (2), we obtain the equation for the time dependence of true anomaly $v(t)$ in the form

$$p^{3/2} K^{-1/2} \int_0^{v(t)} [1 + e \cos v]^{-2} dv = t. \tag{3}$$

Due to the condition $v(t) = 0$ at $t = 0$, equation (3) determines the time of motion from the pericenter to the point of orbit with the given value of anomaly $v(t)$. The trivial case $e = 0$ corresponds to the uniform motion by the circular orbit. In the case $e = 1$ at $\mathscr{E} = 0$ the motion occurs by the parabolic orbit, and equation (3) takes the form

$$\tan \frac{v}{2} + \frac{1}{3} \tan^3 \frac{v}{2} = \frac{2K^{1/2}t}{p^{3/2}} = \frac{2\pi t}{T_p} = t_p. \tag{4}$$

$T_p = \pi K^{-1/2} p^{3/2}$ is the characteristic time scale, which is an independent value and corresponds to the motion on the interval p. Equation (4) is known as the Barger equation [1, 2]. It has an exact analytical solution,

$$v(t) = 2 \arctan\big\{[(1 + S^2(t))^{1/2} + S(t)]^{1/3} - [(1 + S^2(t))^{1/2} - S(t)]^{1/3}\big\},$$

where $S(t) = 3p^{-3/2} K^{1/2} t$.

As can be easily verified, $v(t)$ has asymptotics

$$v(t) \to \begin{cases} \frac{4}{3} S(t) & \text{at} \quad t \ll T_p, \\ 2 \arctan(2S(t))^{1/3} & \text{at} \quad t \gg T_p. \end{cases}$$

The integral in equation (3) at $0 < e < 1$ is also expressed in elementary functions, as the result we obtain the well-known relation

$$\left(\frac{1-e}{1+e}\right)^{1/2}\tan\frac{v}{2}=\tan\left\{\frac{t_*}{2}+\frac{e}{2}(1-e^2)^{1/2}\frac{\sin v}{1+e\cos v}\right\}, \tag{5}$$

in which $t_* = 2\pi t/T$, $T = 2\pi a^{3/2}K^{-1/2}$ is the orbital period, $a = p(1-e^2)^{-1}$ is the semi-major axis of ellipse, the independent parameters are a and e. Equation (5) is the transcendental and its exact analytical solutions are unknown. It is possible to use numerical methods. To find an approximate analytical solutions at small values of eccentricity iterative methods can be used, putting in zero approximation $v(t_*) = t_*$, which means replacing the elliptical orbit with the circular one ($e = 0$).

Another approach makes use of substitution

$$\left(\frac{1-e}{1+e}\right)^{1/2}\tan\frac{v}{2}=\tan\frac{E_e}{2}, \tag{6}$$

where E_e is an auxiliary function, the so-called eccentric anomaly. As the result, equation (5) is significantly simplified and takes the form [2,3]

$$E_e - e\sin E_e = t_*. \tag{7}$$

This is Kepler's equation with unknown in the finite form analytical solutions. Functions $v(t_*)$ and $E_e(t_*)$ are periodic functions of time with period 2π at the elliptical motion, therefore, it is sufficient to consider solutions of equations (5) and (7) on the interval $0 \leqslant t_* \leqslant 2\pi$. The advantage of usage of equation (7) consists in that the deviation $E_e(t_*)$ from zero approximation $E_0(t_*) = t_*$ is much smaller than the deviation $v(t_*)$ from $v_0(t_*) = t_*$.
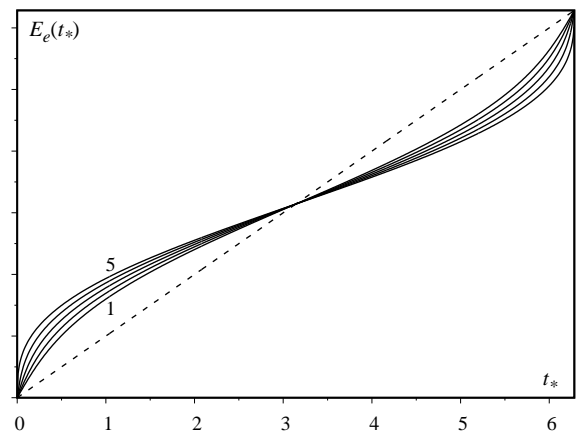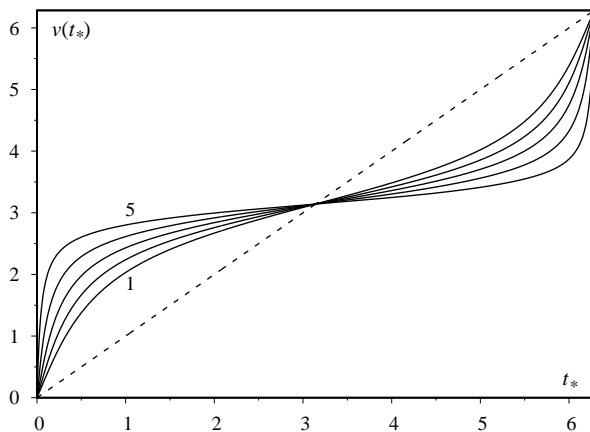
Fig. 1. Dependence of true anomaly $v(t_*)$ on time at different values of eccentricity e (curve $1 - e = 0.5$, $5 - e = 0.9$; $\Delta e = 0.1$). Dashed curve $- e = 0$.

Fig. 2. Dependence of eccentric anomaly $E_e(t_*)$ on time at different values of eccentricity e (curve $1 - e = 0.6$, $5 - e = 1.0$; $\Delta e = 0.1$). Dashed curve $- e = 0$.

Solutions of equations (5) and (7) obtained by the numerical method are shown in Figures 1 and 2.

The most well-known methods of finding approximate analytical solutions of Kepler's equation are the iterative Lagrange method (expansions by powers of eccentricity) and Fourier series method. As one can see from expression (6), functions v and E_e coincide at $e = 0$. In Lagrange method, zero approximation is choosing $E_e(t_*) = t_*$, that corresponds to the circular orbit, and solution of equation (7) is represented by the infinite series [3]

$$E_e(t_*) = t_* + \sum_{k=1}^{\infty}\frac{e^k}{k!}\frac{d^{k-1}}{dt_*^{k-1}}\{\sin^k t_*\}.$$

Functions $\sin E_e(t_*)$, $\cos E_e(t_*)$, $v(t_*)$ are represented similarly. As was shown by Laplace, expansions by powers of eccentricity coincide absolutely only in the region $0 < e < \bar{e} = 0.66274\ldots$ (see [3]).

Using Fourier series expansion, solution (7) takes the form [3]

$$E_e(t_*) = t_* + \sum_{k=1}^{\infty} \frac{2}{k} I_k(ke) \sin(kt_*),\qquad(8)$$

where $I_k(ke)$ are Bessel functions of an integer order of the first kind [4]

$$I_k(ke) = \frac{1}{\pi} \int_0^{\pi} \cos[k(z - e\sin z)]dz.$$

In case when values of e, are close to unit and values of t_* are small, series (8) is convergent weakly and requires taking into account dozens of terms. That's why method is cumbersome and irrational.

Exact solutions of Kepler's equation obtained with help of complex variable functions should be considered to prove this equation solutions [5, 6] existence. They are too much cumbersome and inconvenient for practical use and demand numerical calculations of the quadratures, appearing in solutions. We propose simple and fast-convergent analytical iterative algorithms, which are convenient to use, based on the renormalized perturbation theory — an universal method of modern theoretical physics.

2. The approximate analytical images of Kepler's equation solutions

The time dependence of eccentric anomaly in general terms is illustrated in Figure 2. One can notice, that $E(t_*)$ is a monotonically increasing function of time, and its derivatives in the vicinity of points $t_* = 0$ and $t_* = 2\pi$ are big. From equation (7) follows, that on the interval $\pi \leqslant t_* \leqslant 2\pi$

$$E_e(t_*) = 2\pi - E_e(2\pi - t_*),$$

therefore, it is enough to find solutions in the region $0 \leqslant t_* \leqslant \pi$.

To find the approximate analytical solutions of equation (7), we will apply the following algorithm of successive approximations, which is suitable in the whole region $0 < e \leqslant 1$. For this purpose, let us rewrite equation (7) in the form

$$E_e(t_*) - e\sum_{k=0}^{k_0}(-1)^k \frac{E_e^{(2k+1)}(t_*)}{(2k+1)!} = t_* + ef_{k_0}(E_e(t_*)),\qquad(9)$$

where

$$f_{k_0}(E_e(t_*)) = \sin E_e(t_*) - \sum_{k=0}^{k_0}(-1)^k \frac{E_e^{(2k+1)}(t_*)}{(2k+1)!},$$

$f_{\infty}(E_e(t_*)) = 0$. For zero approximation $E_e^{(0)}(t_*)$ we choose the solution of equation (9) at $f_{k_0}(E_e(t_*)) = 0$. Substituting $E_e^{(0)}(t_*)$ into the right-hand side of equation (9), we obtain equation of the first approximation and etc.

The simplest option of solution is realized at $k_0 = 1$, and equation of zero, the first and other approximations are cubic. According to Cardano's formulae, we obtain

$$E_e^{(0)}(t_*) = \left\{ \left[q_0^3 + s_0^2\right]^{1/2} + s_0 \right\}^{1/3} - \left\{ \left[q_0^3 + s_0^2\right]^{1/2} - s_0 \right\}^{1/3},$$

$$q_0 = \frac{2}{e}(1 - e), \quad s_0 = \frac{3}{e}t_*;\qquad(10)$$

$$E_e^{(1)}(t_*) = \left\{ \left[q_0^3 + s_1^2\right]^{1/2} + s_1 \right\}^{1/3} - \left\{ \left[q_0^3 + s_1^2\right]^{1/2} - s_1 \right\}^{1/3},$$

$$s_1 = \frac{3}{e}\left\{ t_* + ef_1\left(E_e^{(0)}(t_*)\right) \right\},\qquad(11)$$

and etc. Such algorithm has a good convergence. In the region $t_* \lesssim 1$ the approximation $E_e^{(0)}(t_*)$ is close to the solution calculated numerically, and $E_e^{(0)}(t_*)$ has the following asymptotics for small values of t_*

$$E_e^{(0)}(t_*) \Rightarrow \begin{cases} \dfrac{t_*}{1-e} + \ldots & \text{at} \quad t_* < \dfrac{e}{3}\left[\dfrac{2}{e}(1-e)\right]^{3/2}, \\[2ex] \left(\dfrac{6}{e}t_*\right)^{1/3} + \ldots & \text{at} \quad t_* > \dfrac{e}{3}\left[\dfrac{2}{e}(1-e)\right]^{3/2}. \end{cases}$$

In the particular case $e = 1$

$$E_1^{(0)}(t_*) = (6t_*)^{1/3} \tag{12}$$

at all values of t_* with the region $0 \leqslant t_* \leqslant \pi$. The time dependence of eccentric anomaly in different approximations is shown in Figure 3 for $e = 0.8$.
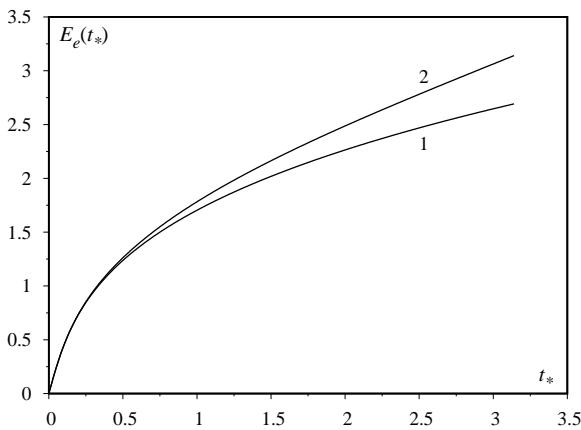
Fig. 3. The time dependence of eccentric anomaly $E_e(t_*)$ in different approximation at $e = 0.8$. Curve 1 corresponds to approximation (10), curve 2 — (11).

Zero approximation $E_e^{(0)}(t_*)$ at $k_0 = 1$ corresponds to the curve 1. The first iteration $E_e^{(1)}(t_*)$ represents the curve 2, which coincides with the results obtained numerically. Such approximation is sufficient for the calculation at all values of eccentricity $e < 1$.

Case $e = 1$ is special one, therefore, we used another iteration method. In the role of zero approximation is given function (12). Substituting it under the sine sign in equation (7), we obtain the following approximation

$$E_1^{(1)}(t_*) = t_* + \sin E_1^{(0)}(t_*).$$

To improve the convergence of iterative process in the role of new zero approximation we use the expression

$$0.5\left\{E_1^{(0)}(t_*) + E_1^{(1)}(t_*)\right\} = \tilde{E}_1^{(0)}(t_*),$$

which is close to solution obtained numerically. The higher approximation we find by the method of ordinary iterations, according to the relation

$$\tilde{E}_1^{(n+1)}(t_*) = t_* + \sin(\tilde{E}_1^{(n)}(t_*)), \quad n \geqslant 0.$$

Taking to account asymptotics (12), the solution obtained by the iterations method can be approximated by the expression

$$E_1(t_*) = \frac{6^{1/3}t_*^{1/3} + a_1 t_* + a_2 t_*^2}{1 + b_1 t_* + b_2 t_*^2} \tag{13}$$

at coefficients $a_1 = 0.0905079$, $a_2 = -0.00772944$; $b_1 = -0.0134609$, $b_2 = -0.00448793$. It deviates from the solution obtained by numerical method no more than 0.003%.

Analytical solutions of Kepler's equation also can be obtained using other iterative algorithms and their combinations. For example, we consider the algorithm that allows to represent the solution in the form of the functional continued fraction. For this purpose, we will rewrite Kepler's equation in the form

$$E_e(t_*) = \frac{t_*}{1 - e[E_e(t_*)]^{-1}\sin E_e(t_*)}. \tag{14}$$

Choosing some kind of function $E_e^{(0)}(t_*)$ in the role of zero approximation, we will calculate the following iterations according to the rule

$$E_e^{(n+1)}(t_*) = \frac{t_*}{1 - e\left[E_e^{(n)}(t_*)\right]^{-1}\sin E_e^{(n)}(t_*)}, \quad n \geqslant 0.$$

The solution arises in the form of continued fraction of the finite order [7]. The main theorem of continued fractions verifies, that the exact solution of equation of type (14) is between n-th and $(n+1)$-th fractions. To improve the convergence of iterative process, let's choose in the role of zero

approximation for equation (14) the linear combination

$$\tilde{E}_e^{(0)}(t_*) = aE_e^{(n)}(t_*) + bE_e^{(n+1)}(t_*), \qquad (15)$$

where positive coefficients satisfy the condition $a + b = 1$. Next, the solution would be according to the scheme

$$\tilde{E}_e^{(n+1)}(t_*) = \frac{t_*}{1 - e\left[\tilde{E}_e^{(n)}(t_*)\right]^{-1}\sin \tilde{E}_e^{(n)}(t_*)}, \quad n \geqslant 0. \qquad (16)$$

In Figure 4 curve 1 represents the function $E_1^{(0)}(t_*) = (6t_*)^{1/3}$, curve 2 — the function

$$E_1^{(1)}(t_*) = \frac{t_*}{1 - \left[E_1^{(0)}(t_*)\right]^{-1}\sin E_1^{(0)}(t_*)}. \qquad (17)$$

Curve 3 represents function (15) at $a = b$,

$$\tilde{E}_1^{(0)}(t_*) = 0.5\left\{E_1^{(0)}(t_*) + E_1^{(1)}(t_*)\right\}. \qquad (18)$$

Curve 4 corresponds to function $\tilde{E}_1^{(1)}$ calculated by formulae (16), (18). Dashed curve represents function (15) choosing the coefficients according to the rule of "golden section",

$$\tilde{\tilde{E}}_1^{(0)}(t_*) = aE_1^{(0)}(t_*) + (1 - a)E_1^{(1)}(t_*), \qquad (19)$$

where $a = 0.5(\sqrt{5} - 1)$. Functions $\tilde{E}_1^{(1)}(t_*)$ and $\tilde{\tilde{E}}_1^{(0)}(t_*)$ practically coincide with each other and with function (13). Therefore, choosing the coefficients according to the rule of "golden section", there is no need to calculate higher iterations.

Fig. 4. Eccentric anomaly at $e = 1$ in different approximations. Curve 1 corresponds to formula $E_1^{(0)}(t_*) = (6t_*)^{1/3}$, curve 2 — (17), curve 3 — (18), curve 4 — (16), (18), dashed curve — (19).

Eccentric anomaly $E_e(t_*)$ is the monotonically varying function of eccentricity. It makes possible to simplify the construction of its analytical images at the large value of eccentricity, using the expansion of function $E_e(t_*)$ into Taylor series in the vicinity of value $e = 1$:

$$E_e(t_*) = E_1(t_*) + (e - 1)\left\{\frac{dE_e(t_*)}{de}\right\}_{e=1} + \frac{(e-1)^2}{2!}\left\{\frac{d^2E_e(t_*)}{de^2}\right\}_{e=1} + \dots.$$

Derivatives by eccentricity can be calculated using equation (7). Taking into consideration that

$$\frac{dE_e(t_*)}{de} = \frac{\sin E_e(t_*)}{1 - e\cos E_e(t_*)},$$

$$\frac{d^2E_e(t_*)}{de^2} = -\frac{\sin E_e(t_*)}{[1 - e\cos E_e(t_*)]^3}\left\{e(1 + \cos^2 E_e(t_*)) - 2\cos E_e(t_*)\right\}, \dots$$

and passing to the limit $e \to 1$, we obtain the following expansion by powers of multiplier $(1 - e)$:

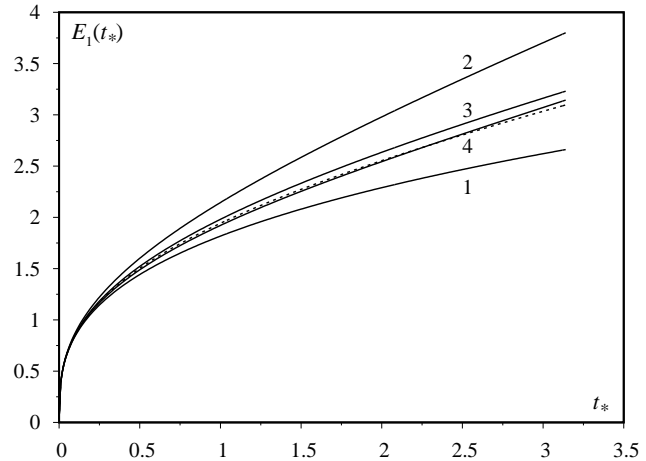$$E_e(t_*) = E_1(t_*) - (1 - e)\frac{\sin E_1(t_*)}{1 - \cos E_1(t_*)} - \frac{1}{2!}(1 - e)^2\frac{\sin E_1(t_*)}{1 - \cos E_1(t_*)} + \dots. \qquad (20)$$

Even better results obtained, when function (20) applied in the region $t_*^e \leqslant t_* \leqslant \pi$, and in the region $0 \leqslant t_* \leqslant t_*^e$ applied expression (10). The universal function $E_1(t_*)$ corresponds to the limiting case of elliptical motion, when the trajectory is the straight line, as the ellipse degenerates.
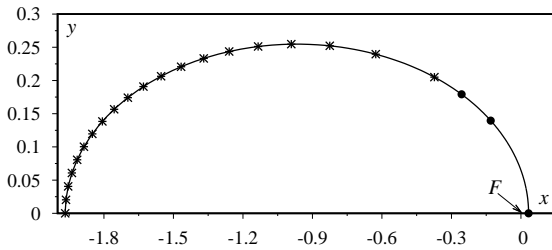
According to relation (6) and relations

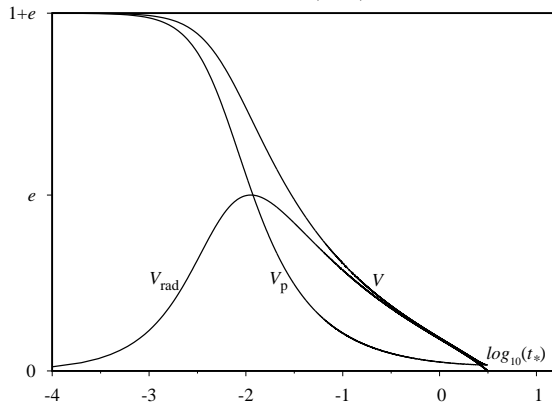$$\cos v(t_*) = \frac{\cos E_e(t_*) - e}{1 - e\cos E_e(t_*)},$$

$$\sin v(t_*) = \frac{E_e(t_*) - t_*}{1 - e\cos E_e(t_*)} \cdot \frac{(1 - e^2)^{1/2}}{e}$$

Fig. 5. The position of Halley's comet on the orbit during half period. The focus of the orbit F is at the origin $(0, 0)$.

Fig. 6. Dependence of the radial and the transversal components, as well as the module of velocity in units $(K/p)^{1/2} \cong 27.56\,\text{km/s}$ on the dimensionless time.

the analytical expression for eccentric anomaly also gives the possibility to calculate in the analytical form true anomaly, polar and cartesian coordinates of a point on the orbit, velocity projections, etc. As an example in Figure 5 it is shown the orbit of Halley's comet (orbital period $T = 76$ years, semimajor axis of the orbit $a = 17.942$ a.u., eccentricity $e = 0.967\ldots$) and its position on the orbit during half period with the interval 1.9 year, marked with asterisks. But the interval between the first three points from the pericenter is equal 0.6333 year.

The time dependence of the radial component of velocity is shown in Figure 6

$$V_{\text{rad}}(t) = \left(1 - e^2\right)^{1/2} e \frac{\sin E(t_*)}{1 - e \cos E(t_*)} \left(\frac{K}{p}\right)^{1/2},$$

the transversal component

$$V_{\text{p}}(t) = \left(1 - e^2\right) \frac{1}{1 - e \cos E(t_*)} \left(\frac{K}{p}\right)^{1/2},$$

as well as the module of velocity

$$V \equiv |\mathbf{V}| = \left(1 - e^2\right)^{1/2} \left[\frac{1 + e \cos E(t_*)}{1 - e \cos E(t_*)}\right]^{1/2}$$

of Halley's comet during half period in units $(K/p)^{1/2} \cong 27.56\,\text{km/s}$.

3. Estimation of the mass of binary system of Galaxy + NGC 224

One way to estimate the mass of binary galaxies is based on models of their relative motion. Since only the radial component of the relative velocity is known from observations, therefore in [8–10] was used model of degenerate elliptical motion with eccentricity $e = 1$. It is assumed in this model, that the Galaxy and NGC 224 are physical connected system, and at the time of their formation they were nearby. Later they divergence for a certain maximal distance $r_{\max}$ having reached to the apocenter. Then began to converge, according to modern observations. In such type model, the motion of galaxies corresponds to the one-dimensional oscillatory process with an amplitude $r_{\max}/2$. In the present era the first period of this process is coming to final. Herewith, the relative radial velocity $V_{\text{rad}}(t) = -123\,\text{km/s}$, distance between galaxies $r(t) = 770\,\text{kpc}$, time is equal to the age of the Universe ($t = 13.7 \cdot 10^9$ years). Based on Kepler's equation for the case $e = 1$ and mentioned above observed data in [8–10] there were assessments the masses sum of these galaxies. It is associated with the mass of Local System in general. The method used in the cited works is known as the "timing argument" method. It is used in modern studies of other binary galaxy systems [11].

However, the assumption about one-dimensional motion of system of these galaxies is not clear. The relative motion by the elliptical orbit with eccentricity close to unit, in general is more likely than the motion by the straight line with zero angular momentum. In this paper we consider the model of non-degenerate elliptical relative motion of galaxies, where the eccentricity is a free parameter and varies in the region $0.6 \leqslant e \leqslant 1.0$, and eccentric anomaly is determined by formulae (7) and (20).

The distance between galaxies at the time moment t

$$r(t) = a\{1 - e \cos E(t_*)\}, \tag{21}$$

where

$$t_* = \frac{2\pi t}{T}, \quad T = 2\pi a^{3/2}(GM)^{-1/2}, \tag{22}$$

M denotes the sum of galaxies masses, and eccentric anomaly is determined by equation (7). According to the accepted model, at the moment of the maximal distance of galaxies (when $E(\tilde{t}_*) = \pi$)

$$r_{\max} = a(1 + e), \tag{23}$$

therefore, equation (21) is rewritten in the form

$$r(t) = \frac{r_{\max}}{1 + e}\big\{1 - e\cos E(t_*)\big\}. \tag{24}$$

The radial component of velocity of relative motion at the time moment t

$$V_{\mathrm{rad}}(t) = \frac{dr(t)}{dt} = \frac{r_{\max}}{1 + e}e\sin E(t_*)\frac{dE(t_*)}{dt} = \frac{r_{\max}}{1 + e}e\sin E(t_*)\frac{1}{1 - e\cos E(_*)}\frac{t_*}{t}.$$

According to equation (24) for the moment of time t

$$V_{\mathrm{rad}}(t)\frac{t}{r(t)} = \frac{t_* e\sin E(t_*)}{[1 - e\cos E(t_*)]^2}. \tag{25}$$

Using observed data $V_{\mathrm{rad}}(t)$ and $r(t)$ in the modern era (at $t = 13.7 \cdot 10^9$ years), equation (25) is rewritten in the form

$$\frac{t_* e\sin E(t_*)}{[1 - e\cos E(t_*)]^2} = -2.23661\ldots. \tag{26}$$

Analytical image of $E(t_*)$ allows us to find t_*^0 being the root of equation (26) as function of the eccentricity (see Table 1), as well as to calculate $E(t_*^0)$.

Table 1. Dependence of the sum of galaxies masses, eccentric anomaly and characteristic times on the eccentricity.

e	t_*^0	$E(t_*^0)$	$M[10^{12}M_\odot]^{-1}$	$t_{\max} = \pi t/t_*^0$, 10^9 y.	$2t_{\max} - t$, 10^9 y.
0.6	5.04837	4.46643	9.06078	8.52549	3.35098
0.7	5.05025	4.38698	7.44792	8.52231	3.34463
0.8	5.07347	4.33096	6.30248	8.48332	3.26664
0.9	5.1102	4.28949	5.44305	8.42233	3.14466
1.0	5.15615	4.25774	4.77373	8.34728	2.99455

To find galaxies mass we use Kepler's equation (7) for t_*^0, definition (22) and relations (23) and (24). As a result, we find that

$$M = \frac{r^3(t)}{G}\big\{1 - e\cos E(t_*^0)\big\}^{-3}\left(\frac{t_*^0}{t}\right)^2.$$

Since the dimensionless time of maximal divergence of galaxies according to Kepler's equation $t_*^{\max} = \pi$, then the absolute time of divergence

$$t_{\max} = \frac{T}{2} = \frac{\pi t}{t_*^0}.$$

Difference $2t_{\max} - t$ determines the time to the future "collision" of galaxies. As was shown in Table, all characteristics (except for t_*^0) are monotonically decreasing functions of eccentricity. The strongest dependence of eccentricity has the sum of galaxies masses, decreasing almost two times at increasing of the eccentricity from 0.6 to 1.0, while time to collision — only on 12%.

For comparison, we represent the estimate of mass obtained by other authors in the model with one-dimensional motion: $(3 \div 6) \cdot 10^{12}\,M_\odot$ [9], $(3.8 \div 6.8) \cdot 10^{12}\,M_\odot$ [10]. In the book [12], where considered the standard model with $e = 1$ was obtained the value $4.83 \cdot 10^{12}\,M_\odot$. In [13] it was shown, that the consideration of non-radiality of relative motion of galaxies significantly affects on the value of total mass, validating our results.

4. Conclusions

Kepler's equation is one of the main relations in celestial mechanics, which determines the relevance of the problem solving. The classical Lagrange method is the conventional perturbation theory, where zero approximation is the solution of linear equation and corresponds to the motion by the circular orbit.

The iterative algorithm proposed by authors can be called as the renormalized perturbation theory, where zero approximation is the solution of non-linear (in the simplest case — of cubic) equation. This leads to the significant reduction of perturbation and fast convergence, when it is enough to take into account one or two iterations.

Representation of Kepler's equation in form (14) and the usage of renormalized perturbation theory allows to obtain solutions in the form of functional fractions of the finite order with fast convergence.

The analytical form of Kepler's equation solutions is convenient for practical usage. It was illustrated by calculations of the time dependence of true anomaly and kinematic characteristics of object motion by the elliptical orbits with large eccentricity using as an example Halley's comet with eccentricity $e = 0.967$. The generalized model of relative motion of binary system of galaxies proposed in paper is another example of usage of Kepler's equation. For the first time, it was studied the dependence of the model characteristics on the eccentricity value.

[1] Barger V., Olsson M. Classical mechanics: A Modern Perspective. McGraw-Hill (1995).

[2] Vallado D. A., McClain W. D. Fundamentals of Astrodynamics and Applications. Microcosm Press (2001).

[3] Alexandrov Yu. V. Celestial Mechanics. V. N. Karazin Kharkiv National University (2003).

[4] Abramowitz M., Stegun I. A. Handbook of Mathematical Functions With Formulas, Graphs, and Mathematical Tables. Government Printing Office Washington (1972).

[5] Siewert C. E., Burniston E. E. An exact analytical solution of Kepler's equation. Celestial Mechanics. **6**, 294–304 (1972).

[6] Philcox O. H. E., Goodman J., Slepian Z. Kepler's Goat Herd: An exact solution to Kepler's equation for elliptical orbits. Monthly Notices of the Royal Astronomical Society. **506** (4), 6111–6116 (2021).

[7] Lorentzen L., Waadeland H. Continued Fractions. Atlantis Press Paris (2008).

[8] Kahn F. D., Woltjer L. Intergalactic Matter and the Galaxy. Astrophysical Journal. **130**, 705–717 (1959).

[9] Einasto J., Lynden–Bell D. On the mass of the Local Group and the motion of its barycentre. Monthly Notices of the Royal Astronomical Society. **199** (1), 67–80 (1982).

[10] Li Y.-S., White S. D. M. Masses for the Local Group and the Milky Way. Monthly Notices of the Royal Astronomical Society. **384** (4), 1459–1468 (2008).

[11] Kudrya Yu. Determination of the double galaxies masses by the "timing argument" method. Bulletin of Taras Shevchenko National University of Kyiv. Astronomy. **57**, 6–9 (2018).

[12] Kudrya Yu., Vavilova I. Extragalactic Astronomy, Book 1. Naukova Dumka (2016).

[13] Van der Marel R. P., Fardal M., Besla G., Beaton R. L., Sohn S. T., Anderson J., Brown T., Guhathakurta P. The M31 Velocity Vector. II. Radial Orbit toward the Milky Way and Implied Local Group Mass. Astrophysical Journal. **753** (1), 8 (2012).

Аналітичні зображення розв'язків рівняння Кеплера та їх застосування

Ваврух М., Дзіковський Д., Стельмах О.

Львівський національний університет імені Івана Франка,
вул. Кирила і Мефодія, 8, 79005 Львів, Україна

Запропоновано прості швидкозбіжні алгоритми аналітичного розрахунку ексцентричної аномалії для довільного ексцентриситету $0 < e \leqslant 1$. Для ілюстрацій розраховано кінематичні характеристики комети Галлея як функції часу та виконано оцінку маси системи Галактика + NGC 224 на основі моделі з еліптичним відносним рухом.

Ключові слова: *рівняння Кеплера; ексцентрична аномалія; істинна аномалія; комета Галлея; маса Місцевої системи Галактик.*